Published in final edited form as:

Curr Biol. 2017 August 07; 27(15): 2381–2388.e4. doi:10.1016/j.cub.2017.06.077.

Early integration of temperature and humidity stimuli in the *Drosophila* brain

Dominic D. Frank[1], **Anders Enjin**[2], **Genevieve C. Jouandet**[1], **Emanuela E. Zaharieva**[1], **Alessia Para**[1], **Marcus C. Stensmyr**[2,*], and **Marco Gallio**[1,*]

[1]Department of Neurobiology, Northwestern University, Evanston, Illinois 60208, USA

[2]Department of Biology, Lund University, Lund, Sweden

Summary

The *Drosophila* antenna contains receptor neurons for mechanical, olfactory, thermal and humidity stimuli. Neurons expressing the ionotropic receptor IR40a have been implicated in the selection of an appropriate humidity range [1, 2], but while previous work indicates that insect hygroreceptors may be made up by a ‘triad’ of neurons (with a dry- a cold- and a humid-air responding cell [3]), IR40a expression included only cold- and dry-air cells. Here, we report the identification of the humid-responding neuron that completes the hygrosensory triad in the *Drosophila* antenna. This cell type expresses the *Ir68a* gene, and *Ir68a* mutation perturbs humidity preference. Next, we follow the projections of *Ir68a* neurons to the brain, and show that they form a distinct glomerulus in the posterior antennal lobe (PAL). In the PAL, a simple sensory map represents related features of the external environment with adjacent ‘hot’, ‘cold’, ‘dry’, and ‘humid’ glomeruli -an organization that allows for both unique and combinatorial sampling by central relay neurons. Indeed, flies avoided dry heat more robustly than humid heat, and this modulation was abolished by silencing dry-air receptors. Consistently, at least one projection neuron type received direct synaptic input from both temperature and dry air glomeruli. Our results further our understanding of humidity sensing in the *Drosophila* antenna, uncover a neuronal substrate for early sensory integration of temperature and humidity in the brain, and illustrate the logic of how ethologically relevant combinations of sensory cues can be processed together to produce adaptive behavioral responses

eTOC Blurb

Correspondence: marcus.stensmyr@biol.lu.se or marco.gallio@northwestern.edu.

SUPPLEMENTAL INFORMATION

Supplemental Information includes Supplemental Experimental Procedures and four figures and can be found with this article online at XXX.

AUTHOR CONTRIBUTIONS

D.D.F, A.E., M.C.S. and M.G. conceived and designed the study. D.D.F. performed all imaging experiments except: A.E. performed antibody stainings and confocal microscopy and humidity preference tests. G.C.J implemented and carried out thermo-hygro preference behavior tests. E.E.Z. built fly strains and contributed to two-photon anatomy. A.P. produced and tested transgenic lines. M.G., and M.C.S. analyzed the data and wrote the manuscript with input from all authors.

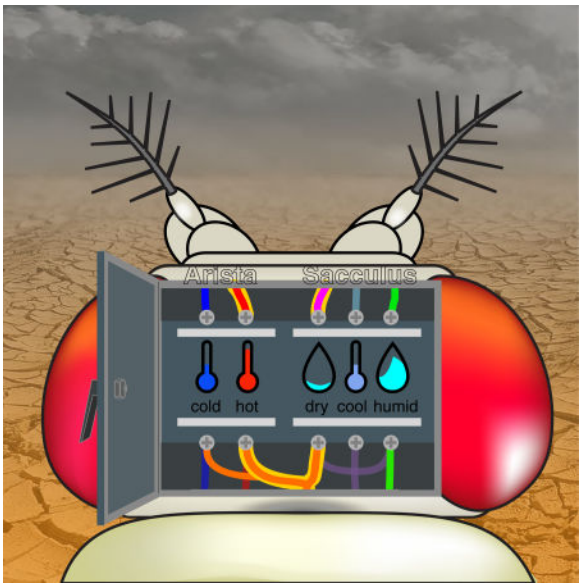

Frank et al. describe humid-air receptors in the fly antenna. Previous work identified dry-air receptors, and they now show that humid and dry cells converge with thermosensory neurons in the brain, creating a sensory map for environmental parameters. They also describe second-order neurons that sample multiple modalities for early integration

Results

Ir68a is expressed in sacculus neurons innervating hygrosensilla

Classic work on insect hygroreceptors suggests that humidity sensing is enabled by dedicated antennal hygrosensilla housing a dry-, a humid-, and a cold- responding neuron [3]. Each cell type in this 'sensory triad' has been suggested to contribute to the detection of changes in air humidity, either by sensing hygroscopic swelling/shrinking of the structure, or by monitoring evaporative cooling [4]. In *Drosophila melanogaster*, we recently identified hygrosensory neurons which innervate the sacculus (a curious invagination of the third antennal segment), and selectively express and require the ionotropic receptor IR40a ([1], see also [2]). *Ir40a* demarcates two populations of sacculus neurons which respond to dry-air stimuli and cooling, respectively [1, 2]. We thus looked for additional *Ir* genes that may show restricted expression in the sacculus, with the immediate goal of finding the missing humid-air responding cell of the 'triad'.

In this search, the *Ir68a* gene emerged as a strong candidate. First, in a phylogenetic tree of the IR family, IR68a grouped with both IR40a and IR93a (the latter also extensively expressed in the sacculus)(Figure 1A). Second, we identified a Gal4 driver derived from the regulatory region of *Ir68a*, which displays narrowly restricted expression in sacculus neurons of chamber I and II (VT029048, from the Vienna Tile collection- hereafter referred to as *Ir68a-Gal4*). To study the expression pattern of *Ir68a*-Gal4 in detail, we first used it to drive the membrane marker CD8:GFP, and analyzed intact antennae by confocal microscopy (Figure 1B). *Ir68a*::*CD8:GFP* prominently labeled neurons innervating chamber II of the

sacculus, and 3D reconstructions demonstrated that these neurons send one dendrite to each of the sensilla housed in this chamber (Figure 1C–F, and see methods for details). This line also inconsistently labeled a small number of cells innervating chamber I sensilla (data not shown). Notably, chamber II sensilla (and some chamber I) have been suggested to contain 3 neurons [5], two of which are accounted for by IR40a-expression. We reasoned that, if *Ir68a*-Gal4 expression demarcated cells that do not also express IR40a, these neurons would be strong candidate humid-air receptors, as they would complete the hygrosensory triad in chamber II.

To test this hypothesis directly, we next used an anti-IR40a antibody and stained antennae from animals that also expressed CD8:GFP under the control of *Ir68a*-Gal4. Indeed, we observed no overlap between the population of cells that were labeled by the IR40a antibody and those expressing *Ir68a*::GFP (see Figure 1C–E and 3D reconstruction in **F**). This implies that the one cell per sensillum labeled by *Ir68a*-Gal4 is distinct from the two cells/sensillum characterized by IR40a expression. We also sought to determine if these newly identified neurons may co-express IR25a. IR25a has been described as an obligatory co-receptor for a number of IRs [6], including IR40a and Ir93a. We thus tested whether IR68a may also be co-expressed with this IR co-receptor. Immunostaining using an anti-IR25a antibody showed, however, little or no overlap with the cell population labeled by *Ir68a::GFP* (Figure 1G–I).

Ir68a expressing neurons respond to humid air stimuli

Our results indicate that *Ir68a*-Gal4 labels a cell population that is distinct from the dry and the cold activated cells that express IR40a, but innervates the same sensilla in chamber II of the sacculus (Figure 1J). This observation alone points to these Ir68a expressing cells as candidates for the missing humid-air cells of the ‘triad’. Do *Ir68a*-expressing neurons indeed respond to humid-air stimuli, and is IR68a required for the physiological and behavioral responses to external humidity?

To answer these questions, we first used *in vivo* calcium imaging and 2-photon microscopy to characterize the physiological responses of *Ir68a* neurons to humid air, dry air, and temperature. Here, we imaged synaptic release from the terminals of *Ir68a* neurons by expressing the transgenic calcium indicator G-CaMP6 [7] under the control of *Ir68a*-Gal4. We then challenged the animal with the chosen stimuli, while recording ensuing activity in the brain. The projection of IR68a-expressing sacculus neurons coalesce in a single ‘bean’ shaped glomerulus in the Posterior Antennal Lobe (PAL, Figure 1K–L); indeed, we observed strong, positive calcium transients in this glomerulus in response to humid-air stimuli of constant temperature (Figure 1M). In contrast, heating and cooling stimuli appeared to have no effect (Figure 1N), while dry-air stimulation resulted in negative calcium transients (which were also evident at the end of a step stimulus of humid-air, Figure 1M).

We next tested behavioral humidity preference in the IR68a insertional mutant, $Ir68a^{MB05565}$. When given a choice between 70% and 20% relative humidity (RH) in a simple 2-choice assay [1], wild-type flies show an initial aversion to the humid side (evident in the first ~15 minutes of the experiment), which is later resolved in a stable choice of 70%

over 20% RH (Figure 1O, and see Figure S1). This initial choice for a preferred humidity range appeared to be perturbed in *IR68a* mutants, as $IR68a^{MB05565}$ flies displayed a reduced initial aversion for the humid side. Nevertheless, $IR68a^{MB05565}$ animals ultimately selected the 70% RH side, similar to controls (Figure 1O, Figure S1).

We have previously reported that *Ir40a* RNAi animals (affecting the responses to dry air) make no choice in this assay even after 4 hours [1]. The starkly different impact on humidity-guided behavior of *Ir40a* vs. *Ir68a* mutations may be due to the fact that dry conditions are likely invariably dangerous and avoided, while humid air may have a more nuanced aversive or attractive valence depending on context.

A simple glomerular map represents external temperature and humidity in the PAL

How is the representation of humid air stimuli integrated with that of dry air, and hot/cold temperature in the brain? We have shown here that, like in other insects, *Drosophila* hygroreceptors are made up of a triad of neurons responding to cold- dry-, and humid air. Rapid temperature responses are instead mediated by dedicated hot and cold thermosensory neurons of the arista, the last antennal segment [8]. Interestingly, humid-, dry-, and cool-responding hygrosensory receptor neurons (HRNs), as well as the thermosensory receptor neurons of the arista (TRNs, [8]), all targeted the Posterior Antennal Lobe (PAL), forming distinct glomeruli adjacent to each other (Figure 2).

To visualize hygrosensory and thermosensory projections within the PAL, we used a number of well-characterized IR drivers and compared the projection of fluorescently labeled terminals using 2-color 2-photon microscopy. As mentioned above, *Ir68a*::GFP neurons target a small glomerulus at the inferior edge of the PAL (the ‘bean’). Co-labeling of IR40a projections (using *Ir40a*-LexA [2] to drive Aop-TdTomato) revealed essentially no overlap (Figure 2A–B). The *Ir40a* positive (*Ir40a+*) glomerulus that responds to dry air (the ‘arm’) delimited the superior profile of the PAL (Figure 2A), while the vertical *Ir40a+* glomerulus that responds to cooling (the ‘column’) laid both dorsal and anterior to *Ir68a+* termini (Figure 2B). *Ir93a*-LexA [9] was active in most (if not all) sacculus neurons innervating chambers I and II, as well as in both hot- and cold- sensing neurons of the arista [9]. As a result, all PAL glomeruli appeared to be innervated by *Ir93a*::TdTomato projections. We also observed GFP/TdTomato co-expression in *Ir68a+* fibers targeting the ‘bean’ (Figure 2 C–D). We note though that the *Ir93a*-LexA driver likely has a broader expression pattern than the endogenous gene, given that sacculus neurons expressing IR93a also express IR40a, which is not expressed in the neuron population targeting the ‘bean’ ([2], Figure 1C–E).

Finally, we tested the broadly expressed co-receptor IR25a. IR25a is expressed (and required) in thermosensory neurons of the arista, as well as (amongst many others) in *Ir40a*-expressing neurons of the sacculus [1]. Our antibody stainings suggest that IR25a is excluded from *Ir68a*-expressing cells (Figure 1G–I) and, consistent with this finding, the *Ir25a*-Gal4 driver was also conspicuously absent from the corresponding region of the PAL (Figure 2E–H).

Hence, the PAL comprises a consolidated spatial representation of multiple related features of the physical environment, with adjacent ‘humid-’, ‘dry-’, ‘hot-’ and ‘cold-’ responding

glomeruli (Figure 2I–N). This spatial arrangement may represent an opportunity for both unique and combinatorial sampling of environmental signals by second-order relay pathways.

Projections neurons of the 'bean' are a substrate for the relay of humid-air responses

To better understand how PAL activity may be processed and relayed to higher brain centers, we searched available collections of Gal4 drivers (the Vienna tile and Janelia FlyLight [10] collections) for lines active in putative second-order relay neurons of the humid- and dry-glomeruli of the PAL.

Olfactory glomeruli of the antennal lobe and thermosensory glomeruli of the PAL are innervated by projection neurons (PNs), whose axons ascend to higher brain centers. Searching for similar cell types, we found two driver lines (R24G07, and VT064570) that labeled 1–2 neurons, which densely innervated the humid-air glomerulus before projecting to the higher brain; we term these cells hygrosensory projection neurons, or hPNs. We choose to further characterize one of these drivers, R24G07, due to its relatively narrow brain expression pattern (Figure S1, and see methods for details), and availability of a LexA variant. These hPNs exclusively innervate the 'bean', and their projections targeted the calyx of the Mushroom Body (MB), as well as the border region between the Lateral Horn (LH) and upper edge of the Posterior Lateral Protocerebrum (PLP) (Figure 3A). We note that this innervation pattern is strikingly similar to that of thermosensory PNs (tPNs) [9].

R24G07 hPNs were indeed direct synaptic targets of humid air hygroreceptors: 2-color 2-photon microscopy demonstrated extensive overlap between axonal termini of *Ir68a*-expressing neurons (labeled by GFP) and R24G07 projections within the 'bean' (expressing TdTomato under R24G07-LexA, Figure 3B). Moreover, GFP-reconstitution across synapses (GRASP, using our activity-dependent synaptobrevin:GRASP system [11]), showed that active synapses exist between the two cell types (Figure 3C), and live 2-photon imaging using G-CaMP confirmed that R24G07 responds to humid air (Figure 3J), but not to temperature stimuli (data not shown) -similar to the *Ir68a*-expressing neurons. Finally, silencing R24G07 cells using Kir2.1 (i.e. by hyperpolarization, [12]) resulted in a phenotype comparable to that of *Ir68a* mutants (Figure 3K). We conclude that the hPNs labeled by R24G07 are likely directly post-synaptic to *Ir68a*-expressing neurons of the sacculus, and specifically transmit information regarding increased humidity to higher brain centers.

Temperature and dry-air signals are integrated by broadly tuned PNs of the PAL

Next, we searched the Gal4 collections for potential PNs of the 'arm', i.e. the glomerulus that responds to dry air. We identified a number of local neurons that appear to innervate the arm (data not shown), but so far no PNs specific for this structure. Instead, we observed that a previously described driver that densely innervates temperature glomeruli of the PAL [9, 13] also targets the arm (Figure 3D–F). This driver, R22C06, is expressed in ~5–8 neurons that receive direct synaptic input from both hot- and cold-sensing neurons of the arista (as demonstrated by syb:GRASP, [9]) and respond to either heating or cooling stimuli [9, 13].

R22C06 neurons also arborize within the dry-air glomerulus, but do not innervate the humid-air glomerulus (Figure3D–E) or the column (data not shown). We note that this is

different from a PN previously recorded in cockroaches, which appears to receive input from all three cell types of the hygrosensory triad [14]. Instead, syb:GRASP demonstrated active synapses between *Ir40a* positive termini in the Bean and R22C06 projections (Figure 3F), and live 2-photon imaging using G-CaMP confirmed that R22C06 cells respond to dry-air stimuli of constant temperature, in a manner similar to the *Ir40a*-expressing neurons (Figure 3J). Importantly, while our preparation does not permit sequential recording of humidity and temperature responses from the same cell (the animal has to be moved to install the temperature stimulation set-up), all ~5–8 individual R22C06 cells have previously been observed to respond to temperature stimuli [9], thus each neuron in this group is likely to integrate activity deriving from hygro- as well as thermosensory neurons.

We have previously shown that this “broadly tuned” cell type is required to mediate avoidance behavior to either hot or cold thermal ranges in a rapid 2-choice assay for temperature preference (including cold temperatures and moderate heat <35°C, [9]). Interestingly, Kir2.1 silencing of R22C06 cells also affected behavioral responses to dry air, so that -when tasked to select between 20% and 70% RH, *R22C06*::*Kir2.1* flies made no choice even after 4 hrs (Figure 3K). This behavioral phenotype is strikingly similar to that previously reported for *Ir40a* RNAi and Kir animals [1]. Therefore, our data indicate that the R22C06 “broadly tuned” neurons are even more broadly tuned than previously anticipated – responding to dry-air stimuli as well as to temperature, and required for behavioral responses to dry air as well as to hot and cold. R22C06 cells may thus provide a cellular substrate for the early integration of temperature and dry-air stimuli in the brain.

Dry and Hot conditions summate to mediate aversive responses

What may be the behavioral significance of such a direct neuronal integration of dry-air and temperature signals from the environment? Small insects such as *Drosophila* are at constant risk of desiccation, and -for example- dry heat may be significantly more dangerous to this small poikilotherm than humid heat.

Testing this notion directly provided a challenge: as relative humidity changes as a function of temperature, it is not practical to keep RH constant throughout the arena while at the same time producing the temperature steps that are required for a temperature preference test. To overcome this limitation, we designed a new assay where flies are given a choice between reference conditions (25°C, 35% RH) and either dry heat (5% RH, 30°C) or humid heat (30°C, 75% RH) in separate trials. We then compared avoidance scores for dry heat or humid heat over reference. This new assay combines our rapid 2-choice assay for temperature preference with a four–field olfactometer [15], i.e. to produce in each quadrant an air plume of constant RH, overlaid atop a floor set at either reference or test temperature (see Figure 4 A–B and methods for details). Note that we chose 30°C as a test temperature, as our previous work shows that it elicits significant behavioral avoidance, which in turn requires the normal function of the TRNs of the arista and of R22C06 PNs [8, 9].

Indeed, when given a choice between either dry-heat or humid-heat and reference conditions, both wild type and control genotypes displayed a clear increase in avoidance when heat was paired with dry, as compared to humid air (Figure 4C). Furthermore, this modulation required *Ir40a* and the activity of IR40a-expressing dry receptor neurons: *Ir40a*

mutants and *Ir40a*::*Kir2.1* animals exhibited normal avoidance of hot and humid conditions, but their avoidance score did not increase when heat was paired with dry air (Figure 4C, and see Figure S3 for additional controls). This result demonstrates that the avoidance of dry and hot conditions can summate to mediate aversive behavioral responses in *Drosophila*, and parallels our observation that both *Ir40a* dry receptors and "hot" TRNs of the arista directly synapse onto R22C06 PNs.

Due to its role in temperature responses, we have previously suggested that R22C06 neurons may relay the common negative valence of heating and cooling stimuli, alerting the animal that the temperature is rapidly veering away from the favorable range [9]. As R22C06 neurons are also required for dry-air responses, we now propose that this cell type may convey an even broader 'alert' message, directly integrating signals from dangerous temperature and humidity conditions. We note that this, to the best of our knowledge, is the first example of cross-modal integration that happens this early, at the level of second-order neurons in an ascending neural pathway for sensory relay.

Discussion

The genus *Drosophila* was formally erected in 1817 by the Swedish entomologist Carl Frederik Fallén to encompass 12 small fly species collected in the surroundings of Lund [16]. The name chosen, i.e. "dew lover", was derived from the Swedish *daggflugor* ("dew fly"), presumably reflecting the habitats in which Fallén caught his specimens ("*in prati humidis & umbrosis*", in humid, shady meadows, Figure S4).

We have shown here that the "dew fly" *D. melanogaster* possesses a sophisticated cellular and molecular machinery to detect changes in external humidity. In the fly antenna, a 'triad' of humid-, dry-, and cold- responding neurons innervates specialized hygrosensilla, located within a small invagination of the third segment (the sacculus). This organization closely matches what has been described in other insect species (from cockroaches to stick insects to bees, [3]), and suggest that a similar architecture may underlie the function of hygrosensory sensilla in all insects.

We (and others) have also shown that hygroreceptor neurons express unique combinations of ionotropic receptors of the IR family [1, 2]. Most interestingly, IR40a expression demarcated dry- and cold- responding cells of the sacculus, while IR68a allowed us to identify the missing humid-air receptors of this triad. The mechanism through which these cells and IR molecules may be able to detect changes in external humidity remains rather mysterious, but it is likely to involve a combination of responses to evaporative cooling (e.g. through the 'cold cell' of the triad), as well as to shrinking/swelling of the unique cuticular structure that makes up the sensillum (Figure 1, which may act as a miniature hygromorph [17]).

Here, we also describe how humid-air stimuli are represented in the brain, and how this representation is integrated with that of dry, hot, and cold. In the posterior antennal lobe (PAL), adjacent 'humid-', 'dry- ', 'hot-', and 'cold-' responding glomeruli are arranged next to each other, comprising a consolidated spatial map of related features of the external environment. 'Sensory maps' are indeed a common feature of early sensory representation

in animals, but their significance for signal processing is not always understood. Moreover, this is the first such map that comprises different (albeit related) sensory modalities.

Our data suggest that this organization may facilitate both unique and combinatorial sampling by central relay neurons. We describe a projection neuron (PN) cell type that only samples signals from the humid air glomerulus and only responds to humid air stimuli. This cell type is reminiscent of 'narrowly tuned' PNs of the thermosensory system that only receive input from either hot or cold temperature receptor neurons, and only respond to either hot or cold stimuli.

We also show that 'broadly tuned' PNs directly integrate signals from dry-air sensors of the sacculus as well as temperature receptors of the arista, and are required for the behavioral responses to both thermal and hygrosensory stimuli. This is a unique example of early integration of different sensory signals, and we probe its significance studying the synergy of dry and heat conditions on avoidance behavior. Our results suggest a simple model where the activity of dry-sensing neurons of the sacculus directly summates with that of hot sensing neurons of the arista to drive R22C06 'broadly tuned' PNs, thus utilizing a single conduit for the relay of dangerous hot and dry conditions that often go hand in hand in the environment. Furthermore, all PNs of the PAL appear to converge on many of the same higher brain targets (MB, LH, PLP), with the potential for additional integration and higher-order processing of these related environmental parameters.

EXPERIMENTAL PROCEDURES

All methods and reagents used are described in STAR methods.

STAR Methods

Contact for Reagent and Resource Sharing

Further information and requests for reagents should be directed to and will be fulfilled by the Lead Contact, Marco Gallio (marco.gallio@northwestern.edu)

Experimental Model and Subject Details

Fly Strains—Flies were reared on cornmeal agar medium in room temperature (24°C). Stocks were obtained from Bloomington Drosophila Stock Center (BDSC) or Vienna Drosophila Resource Center (VDRC). The following flies were used: $w^{1118\ CS}$ (w^{1118} backcrossed to Canton-S for ten generations, kind gift from A. Simon), $IR40a^{1}$ (kind gift from R. Benton; Silbering *et al.* 2016), $IR68a^{MB05565}$ (BDSC 26031), *IR40a-Gal4* (BDSC 41727), *Ir40a-LexA* (kind gift from R. Benton, Silbering *et al.* 2016), *VT029048-Gal4,* (VDRC 207464), *Ir93a-LexA* [2], *IR25a-Gal4* (BDSC 41728), *10XUAS-IVS-mCD8::GFP* (BDSC 32186), *20XUAS-IVS-GCaMP6m* (BDSC 42748), *13XLexAop-IVS-GCaMP6m* (BDSC 44275), *R22C06-Gal4* (BDSC 48974), *R24G07-Gal4* (BDSC 49095), *R24G07-LexA* (BDSC 52726), *UAS-syb:spGFP 1–10* and *AOP-CD4:spGFP 11* (BDSC 64314, [3]), *UAS-Kir2.1* (Baines *et al.* 2001). Stocks used for behavior or live imaging were backcrossed to $w^{1118\ CS}$ for 5 or more generations: $IR68a^{MB05565}$, *IR25a-Gal4, IR40a-Gal4, UAS-Kir2.1.*

To generate *R22C06-LexA* transgenic flies, the *R22C06* enhancer region was PCR amplified (see the FlyLight site for primers) and TA cloned into a pENTR vector and subsequently transferred to a pLexA65Uw destination vector by Gateway cloning. *attP2* was used as the landing site.

To generate *13XLexAop-TdTomato* transgenic flies, the *TdTomato* CDS was PCR amplified and TA cloned into a pENTR vector and subsequently transferred into a pJFRC19-*13XLexAop* destination vector through Gateway cloning. *attP18* was used as the landing site.

Method Details

Imunnofluorescence Staining—Antennae were dissected in phosphate-buffered saline (PBS) and then fixed in fresh 2% paraformaldehyde in PBS for 15 minutes at room temperature. After washing 4× in PBS with 0.5% Triton X-100 (PBST) and blocking in PBST with 5% normal goat serum for one hour, antennae were incubated with primary antibody diluted in PBST with 5% normal goat serum for 2–3 days at 4 degrees on an orbital shaker. After rinsing with PBST 4× for 5 min each, antennae were incubated with secondary antibodies diluted in PBST with 5% normal goat serum for 2 days at 4 degrees on an orbital shaker. After washing 3× in PBST antennae were mounted in Rapiclear 1.47 and imaged immediately. Antennae were mounted in Rapiclear 1.47 (SunJin Lab). Cuticular autofluorescence was excited with a 561 nm laser, emitted light captured with a 575 nm longpass filter. The following antibodies were used in this study: rabbit anti-GFP (1:1000, A11122 Life Technologies), chicken anti-GFP (1:500, ab13970, Abcam), rabbit anti-IR25a (1:200, [6]), guinea pig anti-IR40a (1:200, [2]), mouse anti-nc82 (1:30, DSHB), goat anti-rabbit Alexa 488 (1:500, A11070 Life Technologies), goat anti-chicken Alexa 488 (1:500, A11039, Life Technologies), goat anti-rabbit Alexa 594 (1:500, A11037, Life Technologies) and goat anti-guinea pig Alexa 546 (1:500, A11074, Life Technologies) and donkey anti-mouse Cy3 (1:1000, Jackson 715-165-150).

Fluorescent Microscopy and Image Analysis—For imaging immunofluorescent-stained samples, cuticular autofluorescence was excited with a 561 nm laser and emitted light captured with a 575 nm longpass filter. Imaging was performed on a Zeiss LSM 510 META confocal microscope with a 63× objective at 1024×1024 pixel resolution. Two-color, two-photon imaging of GFP- and TdTomato- labeled neurons was performed on a Prairie Ultima two-photon microscope with a Coherent Chameleon Ti:Sapphire laser, GaAsP PMT and an Olympus 40× 0.9NA water immersion objective at 512×512 pixel resolution and 1× or 2× optical zoom. Maximum projections were obtained from stacks taken at 1μm steps. Images were processed in Fiji.

3D reconstructions—Three-dimensional reconstructions of the sacculus (Figure 1) and of PN pathways on an aligned brain template (Figure 3) were performed as follows (and see [9] and [1]). Image stacks were imported to Amira 5.3.3., where neuronal arborizations were manually segmented. For neuron reconstruction, the Skeleton plugin of Amira was used. 3D reconstructions of axonal tracts were carried out on 3D brain volumes pre-aligned to a

standard brain, available through BrainBase. Semi-automated neurite reconstruction was carried out by Amira on representative ViennaTile driver lines.

Calcium Imaging—Responses to humid or dry-air stimuli were recorded from flies expressing either *UAS-GCaMP6m* or *LexAop- GCaMP6m*. Animals were briefly anesthetized using ice or CO2 and fastened to a custom-built headstage using plastic adhesive tape. A small window was excised through the tape and through the head cuticle, and a drop of freshly prepared artificial hemolymph was then applied on top of the tape providing a liquid column for the dipping lens (note that this liquid is on the opposite side of the tape as the antennae are). The preparation was secured to the stage of a two-photon microscope and an adjustable stimulus port (5mm diameter) was positioned directly next to the fly. The fly was presented with a constant 0.5 LPM 'baseline' flow of humidified air (35% RH) produced by a Sable Systems DG-4 Humidity and Dewpoint Controller and rapid 'humid' or 'dry' stimuli were achieved by diverting the airflow to either an empty flask ('dry', ~5% RH) or one filled with deionized water ('humid', ~85% RH) by using a series of computer-controlled three-way valves (Lee Instruments, response time 2ms) actuated by a sequence of TTL pulses. The humidity and temperature of the airflow were recorded in real-time using a miniaturized combination hygrometer/thermometer installed inline immediately upstream of the stimulus port (resolution 0.01% RH / 0.015°C ; Sensirion). All flies remained viable for the duration of the imaging experiment as was evidenced by regular leg movements and occasional natural behaviors (e.g. grooming).

Calcium imaging of temperature stimuli was performed essentially as previously described [9]. Note that temperature stimuli are delivered in a constant high/saturating humidity regime. Dissections were performed in AHL such that sufficient cuticle surrounding the brain was delicately removed to provide optical access to the PAL. The preparation was then placed in a custom-built chamber, covered with a plastic coverslip, and placed on the two-photon microscope stage. Rapid temperature changes were achieved via a microfluidic device, i.e. controlling the temperature of the medium via a custom-built system consisting of a series of three-way valves (Lee Instruments, response time 2ms) and Peltier elements independently controlling baseline, 'hot' and 'cold' flow, respectively. Temperature in the bath was recorded using a BAT-12 electronic thermometer (Physitemp).

Images were acquired at 256×256 pixels resolution and 2× optical zoom at a rate of 4 Hz on a Prairie Ultima two-photon microscope with a Coherent Chameleon Ti:Sapphire laser, GaAsP PMT, and an Olympus 40× 0.9NA water immersion objective.

Behavioral Experiments—The humidity preference assay in Figure 1O and Figure 3K was performed in a 48-well plate (essentially as in [1]). The wells were filled with a saturated solution of LiCl or NaCl (Sigma-Aldrich). The wells were covered with a polyamide mesh (Sintab Produkt AB) and a polyamide 3d-printed custom frame (i.materialize) was placed on the net to create six lanes. Flies were cold anesthetized before the experiment and then distributed 5–8 flies per lane and covered with a lid. The plates were placed on top of transparent plastic boxes (15 cm high) to avoid heating from the light source (Artograph LightPad A940). Movies were captured with a webcam (Logitech C930e) controlled using a custom script written in Matlab (Mathworks). Flies were manually scored

and a preference index was calculated PI = (# flies on moister side - #flies on drier side)/ total # flies. Humidity was measured using an EK-H4 multiplexer equipped with SHT71 sensors and recorded with the EK-H4 viewer software (Sensirion).

To assess rapid heat avoidance at different relative humidity ranges, we designed a new assay as follows. We modified a 4-field olfactometer [15] so that it could be adapted to fit atop our existing 2-choice temperature preference arena. The olfactometer comprises a four-quadrant star-shaped chamber (Figure 4) in which flies walk freely between four air plumes carrying air of set humidity. A central vacuum port draws air into the system through four intake ports, set up so that the flow rate across each can be equalized by independent flowmeters. Before air enters the exposure chamber, it is routed through either empty vials (and therefore remain at 35% RH, as the chamber resides in a RH-controlled incubator) or through vials containing water or dessicant. The experimental setup is housed in a dedicated temperature and humidity-controlled facility and measurements of airflow relative humidity (made by a Cole Parmer Traceable Hygrometer) were adjusted to compensate for the stimulus temperature within the chamber (dry heat 5%RH, 30°C; humid heat 75%RH, 30°C). In each experiment, groups of 15–20 flies are ice anesthetized and introduced to the chamber under ‘standard’ control conditions (25°C, 40% RH). Following recovery, flies are given a choice between a preferred temperature and an aversive one (30°C) for 3 minutes - which in alternate trials is overlaid by either a dry or humid air plume. For each trial, a video of the flies' positions is acquired using an overhead mounted digital camera at 3.75 frames/ second and an Avoidance Index (AI) is calculated by plotting the flies' positions within the chamber frame-by-frame using the following simple formula: AI= n flies at 25°C - n files at TT°C / Total n of flies. AIs for each frame are then averaged across the experiment (i.e. 675 frames).

IR sequence analysis—The phylogenetic analysis of IR sequences was carried out in Geneious 9.1.2. The tree was constructed from a MAFFT alignment on a curated set of IR genes from *D. melanogaster* [6], followed by tree reconstruction via PHYML.

Quantification and Statistical Analysis

Calcium Imaging Data Analysis—Delta F/F analysis was carried out using custom MATLAB scripts. To calculate change in fluorescence we used the formula Delta $F/F_0 = (F_t - F_0)/F_0$, where F_0 is the baseline fluorescence determined by averaging 20 frames before stimulus onset and F_t is the fluorescent value at a given time. Circular regions of interest (ROIs) of constant area were drawn manually, as appropriate using the overlaid averaged image as a guide. Representative stimulus and Delta F/F response pairs were used to generate average traces in MATLAB. Values across individual trials were averaged and the standard deviation was determined for each timepoint.

Behavior Data Analysis—For the humidity preference assay, significance was tested with one-sample t test, theoretical mean 0, $p < 0.05$ was considered significant, i.e. no asterisk indicate no significant preference. For the 4-field rapid temperature and humidity avoidance assay, dry-heat and humid-heat mean avoidance indexes for each genotype were compared using 2 sample t-test ($p<0.05$) in MATLAB.

Supplementary Material

Refer to Web version on PubMed Central for supplementary material.

Acknowledgments

We wish to thank R. Benton for providing fly strains and reagents, Chao Wei for help with microscopy, Tom Bozza, and members of the Gallio and Stensmyr Labs for valuable comments. Work in the Gallio Lab is supported by NIH grant R01NS086859 (M.G.), the Pew Charitable trust (M.G.), and NIH grant F31NS093873 (D.D.F.). Work in the Stensmyr Lab is funded by the Crafoord Foundation (M.C.S.), Vetenskapsrådet (M.C.S.), Birgit och Sven Håkan Ohlssons Stiftelse (M.C.S.), Astrid och Gustaf Kaleens Fond (A.E.), Kungliga Fysiografiska Sallskapet (A.E.), Wenner-Gren Stiftelse (A.E.).

References

1. Enjin A, Zaharieva EE, Frank DD, Mansourian S, Suh GS, Gallio M, Stensmyr MC. Humidity Sensing in Drosophila. Current biology : CB. 2016; 26:1352–1358. [PubMed: 27161501]
2. Knecht ZA, Silbering AF, Ni L, Klein M, Budelli G, Bell R, Abuin L, Ferrer AJ, Samuel AD, Benton R, et al. Distinct combinations of variant ionotropic glutamate receptors mediate thermosensation and hygrosensation in Drosophila. eLife. 2016; 5
3. H Altner, a, Loftus, R. Ultrastructure and Function of Insect Thermo- And Hygroreceptors. Annual Review of Entomology. 1985; 30:273–295.
4. Tichy H, Loftus R. Hygroreceptors in insects and a spider: Humidity transduction models. Naturwissenschaften. 1996; 83:255–263.
5. Shanbhag SR, Singh K, Singh RN. Fine structure and primary sensory projections of sensilla located in the sacculus of the antenna of Drosophila melanogaster. Cell and Tissue Research. 1995; 282:237–249. [PubMed: 8565054]
6. Abuin L, Bargeton B, Ulbrich MH, Isacoff EY, Kellenberger S, Benton R. Functional Architecture of Olfactory Ionotropic Glutamate Receptors. Neuron. 2011; 69:44–60. [PubMed: 21220098]
7. Chen TW, Wardill TJ, Sun Y, Pulver SR, Renninger SL, Baohan A, Schreiter ER, Kerr RA, Orger MB, Jayaraman V, et al. Ultrasensitive fluorescent proteins for imaging neuronal activity. Nature. 2013; 499:295–300. [PubMed: 23868258]
8. Gallio M, Ofstad TA, Macpherson LJ, Wang JW, Zuker CS. The coding of temperature in the Drosophila brain. Cell. 2011; 144:614–624. [PubMed: 21335241]
9. Frank DD, Jouandet GC, Kearney PJ, Macpherson LJ, Gallio M. Temperature representation in the Drosophila brain. Nature. 2015; 519:358–361. [PubMed: 25739506]
10. Jenett A, Rubin GM, Ngo TT, Shepherd D, Murphy C, Dionne H, Pfeiffer BD, Cavallaro A, Hall D, Jeter J, et al. A GAL4-driver line resource for Drosophila neurobiology. Cell reports. 2012; 2:991–1001. [PubMed: 23063364]
11. Macpherson LJ, Zaharieva EE, Kearney PJ, Alpert MH, Lin TY, Turan Z, Lee CH, Gallio M. Dynamic labelling of neural connections in multiple colours by trans-synaptic fluorescence complementation. Nature communications. 2015; 6:10024.
12. Baines RA, Uhler JP, Thompson A, Sweeney ST, Bate M. Altered electrical properties in Drosophila neurons developing without synaptic transmission. The Journal of neuroscience : the official journal of the Society for Neuroscience. 2001; 21:1523–1531. [PubMed: 11222642]
13. Liu WW, Mazor O, Wilson RI. Thermosensory processing in the Drosophila brain. Nature. 2015; 519:353–357. [PubMed: 25739502]
14. Nishino H, Yamashita S, Yamazaki Y, Nishikawa M, Yokohari F, Mizunami M. Projection neurons originating from thermo- and hygrosensory glomeruli in the antennal lobe of the cockroach. The Journal of comparative neurology. 2003; 455:40–55. [PubMed: 12454995]
15. Semmelhack JL, Wang JW. Select Drosophila glomeruli mediate innate olfactory attraction and aversion. Nature. 2009; 459:218–223. [PubMed: 19396157]
16. Fallen CF. Diptera Sueciae. 1814–1827

17. Reyssat E, Mahadevan L. Hygromorphs: from pine cones to biomimetic bilayers. Journal of the Royal Society, Interface. 2009; 6:951–957.

Highlights

- Fly hygroreceptors are composed of a ‘triad’, with a dry-, a cold- and a humid cell
- Humid sensing neurons require the ionotropic receptor IR68a
- Axons of dry and humid receptors and of thermoreceptors form a combined sensory map
- Second-order projection neurons include mono- and multi-modal cell types

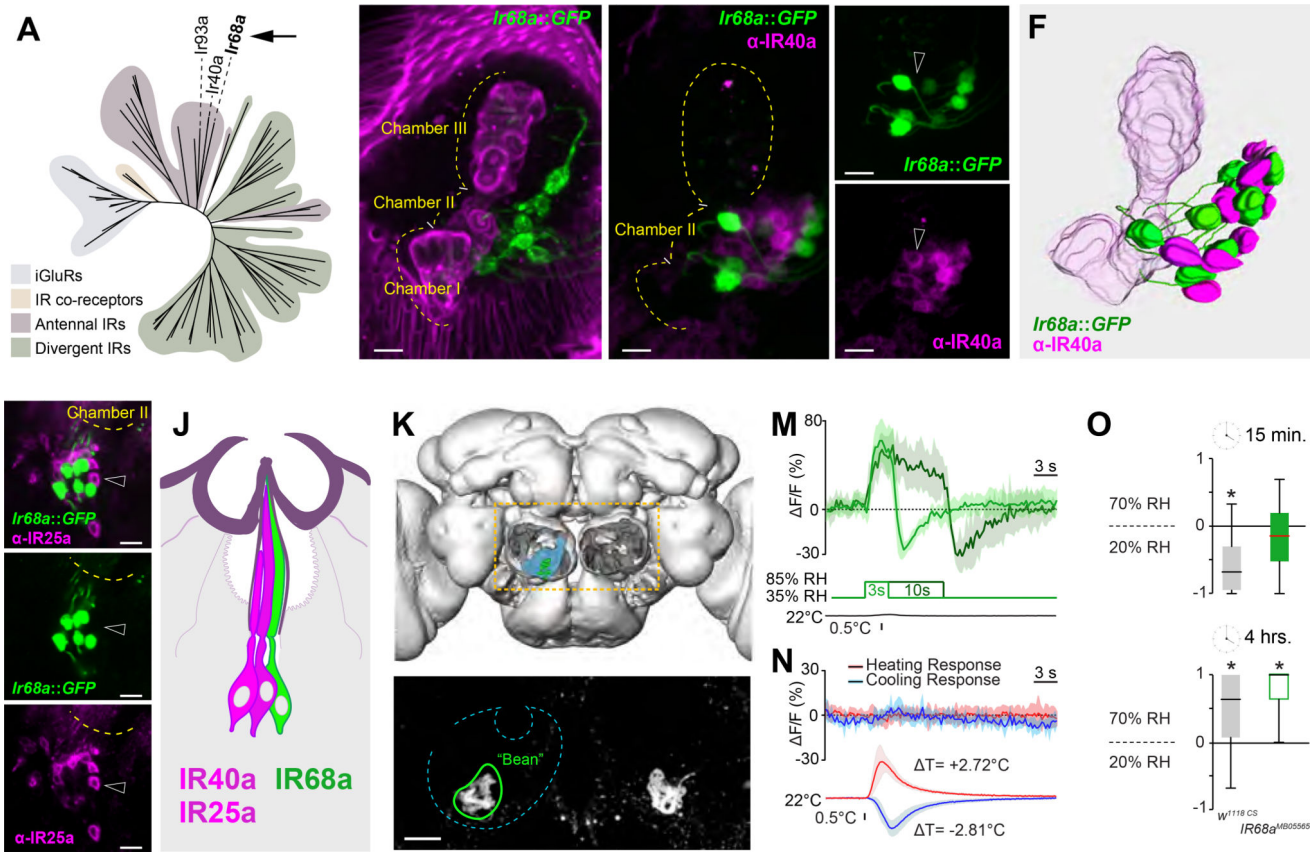

Figure 1. IR68a is expressed in sacculus neurons which mediate humid-air responses

(A) Phylogenetic tree of the IR family, highlighting the position of IR68a.

(B) Ir68a-expressing neurons innervate chamber II of the sacculus, a small invagination of the antenna (Magenta= maximum-intensity projection of cuticular autofluorescence showing the sacculus; green= Ir68a>GFP neurons).

(C–E) Immunostaining of an Ir68a>GFP antenna using anti-IR40a antibodies (max projection of a shallow confocal stack, scalebar=10μm, dotted line=outline of the sacculus, arrowheads point to adjacent cells to highlight no overlap in expression).

(F) 3D model of the sacculus based on (C).

(G–I) Immunostaining of an Ir68a>GFP antenna using anti-IR25a antibodies (max projection of a shallow confocal stack, scalebar=10μm, dotted line=outline of the sacculus, arrowheads point to adjacent cells to highlight no overlap in expression).

(J) Cartoon of a hygrosensory sensillum.

(K) 3D reconstruction of the *Drosophila* brain, antennal lobes removed, to highlight the posterior antennal lobe (PAL, light blue).

(L) 2-photon stack of an Ir68a>GFP brain shows axonal termini converging into two symmetric, 'bean' shaped glomeruli (green outline) in the PAL (scalebar=10μm).

(M–N) Average traces from 'bean' in response to humid air (M) and temperature (N) stimuli (shaded areas represent STD).

(O) Humidity preference index of w^{1118} controls and $Ir68a^{MB05565}$ mutants (see Figure S1 for additional timepoints). The edges of the boxes are the first and third quartiles, thick lines mark the medians, whiskers represent data range. Preference was tested with one-sample t

test, theoretical mean 0, $p < 0.05$ was considered significant, i.e. no asterisk indicate no significant preference.

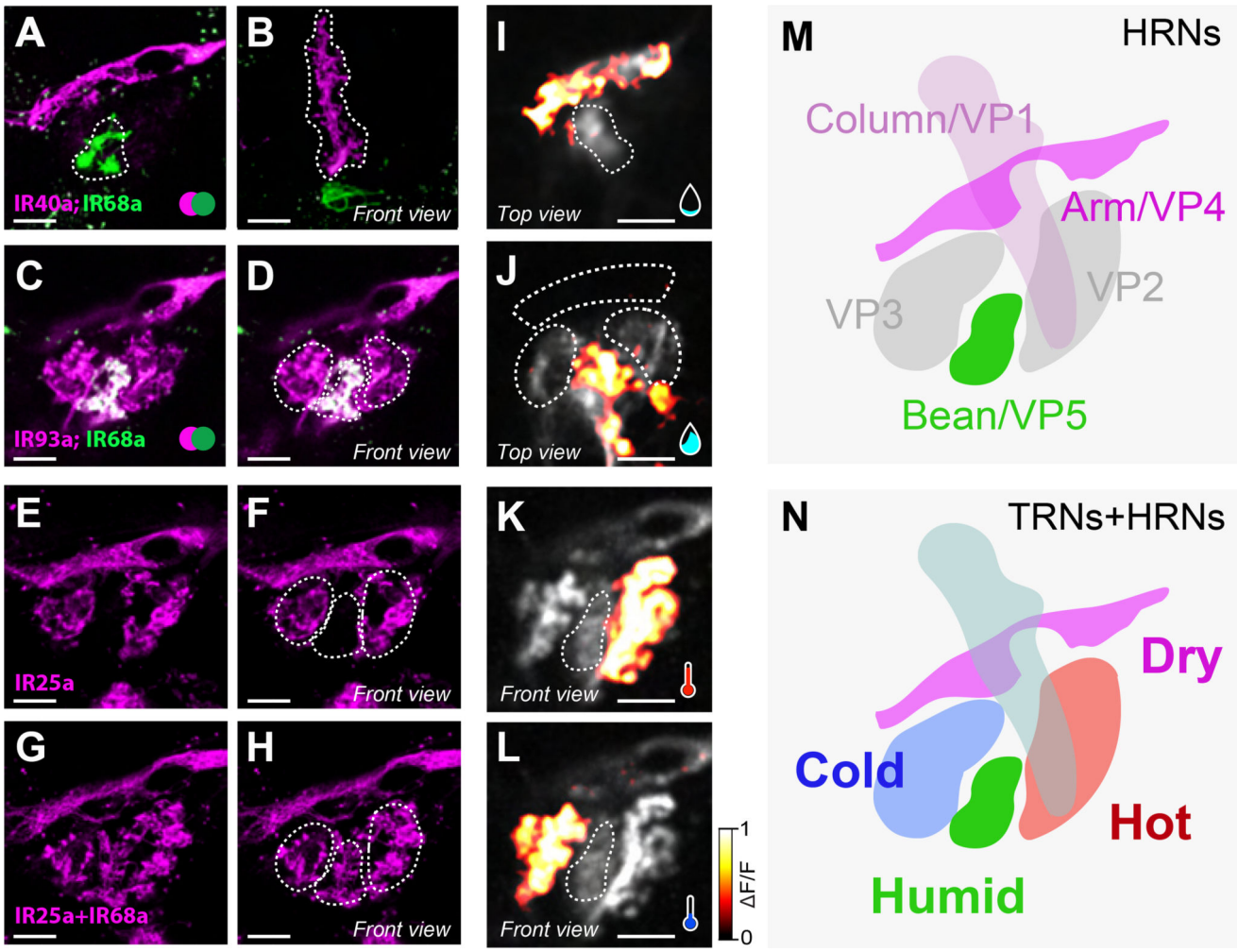

Figure 2. A consolidated map for the representation of temperature and humidity in the fly brain

(A–H) Maximum-intensity projection of 2-color, 2-photon microscopy stacks of transgenically labelled axons innervating humidity and temperature glomeruli in the PAL (green=CD8:GFP, pink=TdTomato). (A–B) Ir68a> CD8:GFP and Ir40a>TdTomato, Arm (A) and Column (B). (C–D) Ir68a> CD8:GFP and Ir93a>TdTomato. (E–F) Ir25a> CD8:GFP. (G–H) Ir68a> CD8:GFP GFP and Ir25a> CD8:GFP. The “Bean” glomerulus is situated between the hot (right) and cold (left) glomeruli, outlined as dotted lines in D, F and H.

(I–L) Calcium responses to humidity and temperatures stimuli recorded in PAL glomeruli expressing G-CaMP6 under the control of the broad IR93a-LexA driver. (I) Arm (but not Column) responds to dry air steps (35% to 5% RH). (J) Bean responds to humid air steps (35% to 85% RH). (K, L) Hot and Cold glomeruli respond to the preferred stimulus (a heating or cooling step of ~2°C). Responses in I and J, K and L were recorded sequentially in the same animal.

(M,N) Map of the spatial configuration of humidity glomeruli from HRNs in the PAL (M) and their relation to the temperature glomeruli (N). Scale bars are 10 μm.

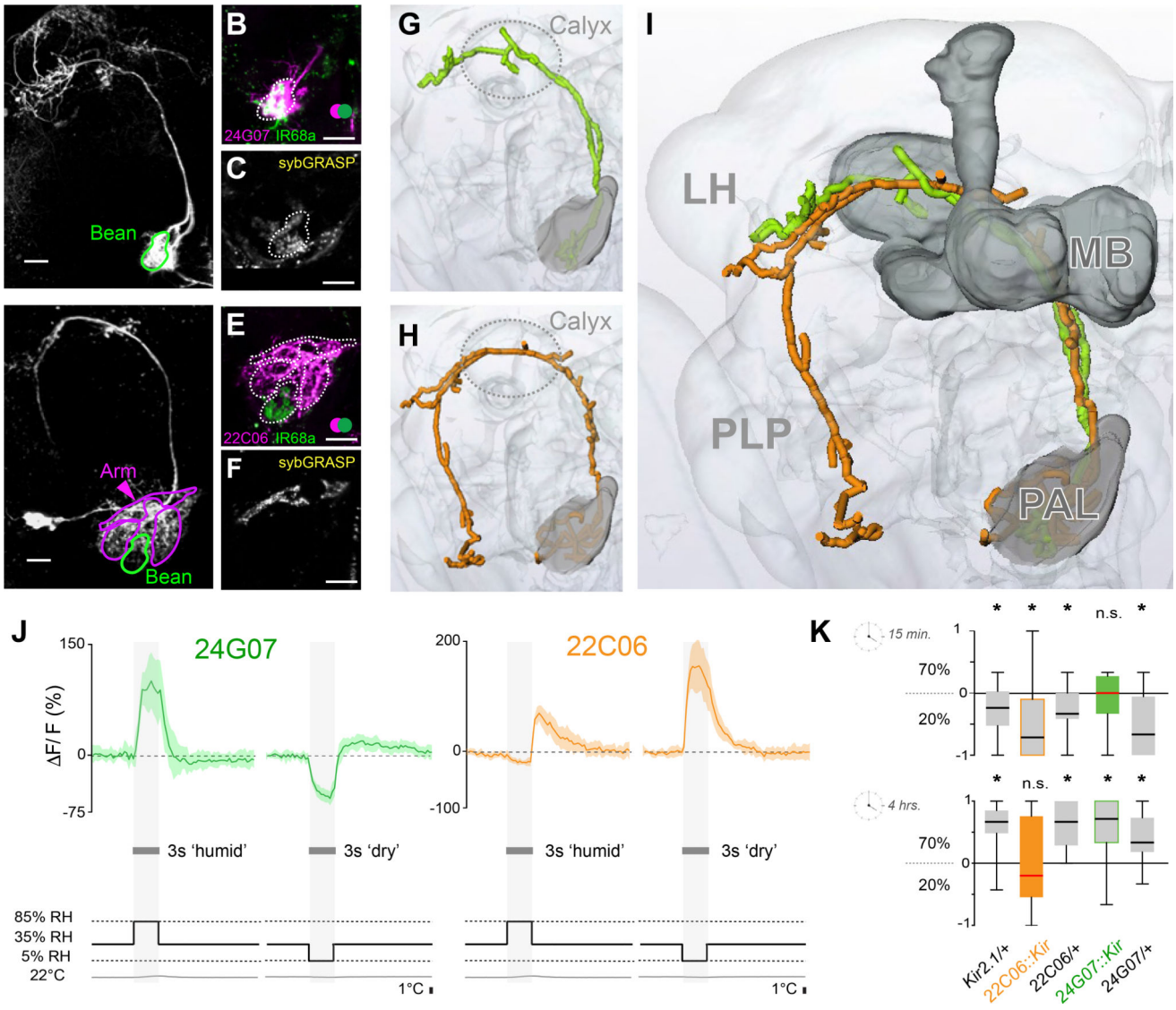

Figure 3. Projection neurons innervating hygrosensory glomeruli of the posterior antennal lobe

(A–F) Maximum-intensity projections of two-photon imaging stacks of live brains expressing transgenic labels (scale bars =10μm). (A) R24G07> CD8:GFP labels hygrosensory PNs innervating the Bean (Se also Figure S2a). (B) R24G07> TdTomato; IR68a> CD8:GFP demonstates significant spatial overlap (green=CD8:GFP, pink=TdTomato; overlap=white). (C) Syb:GRASP GFP reconstitution between IR68a>Gal4 termini and R24G07>LexA projections. (D) R22C06> CD8:GFP labels PNs innervating the Arm, Hot and Cold glomeruli, but not the Bean. (E) R22C06> TdTomato; IR68a> CD8:GFP demonstates no spatial overlap (green=CD8:GFP, pink=TdTomato). (F) Syb:GRASP GFP reconstitution between IR40a>Gal4 termini and R22C06>LexA projections.

(G–I) Three-dimensional reconstruction of the PNs innervating hygrosensory glomeruli. (G) Is a reconstruction of the cell type imaged in A, (H) in D, and (I) is an overlay demonstrating a similar innervation pattern (MB=Mushroom Bodies, LH=Lateral Horn, PLP=Posterior Lateral Protocerebrum; the calyx of the mushroom bodies is circled for reference in G,H).

(J) Averaged calcium traces from R24G07 (green) and R22C06 (orange) PNs in response to humid and dry air stimuli at constant temperature (for each trace n = 3–5 animals, 5 responses, envelope = STD, see also Figure S2b).
(K) Humidity preference behavior of R24G07>Kir2.1 (green), R22C06>Kir2.1 (orange), and genetic background controls (grey) after 15 minutes (top) and 4 hours (bottom). The edges of the boxes are the first and third quartiles, thick lines mark the medians, and whiskers represent data range. Preference was tested with one-sample t test, theoretical mean 0, $p < 0.05$; no asterisks indicate no significant preference.

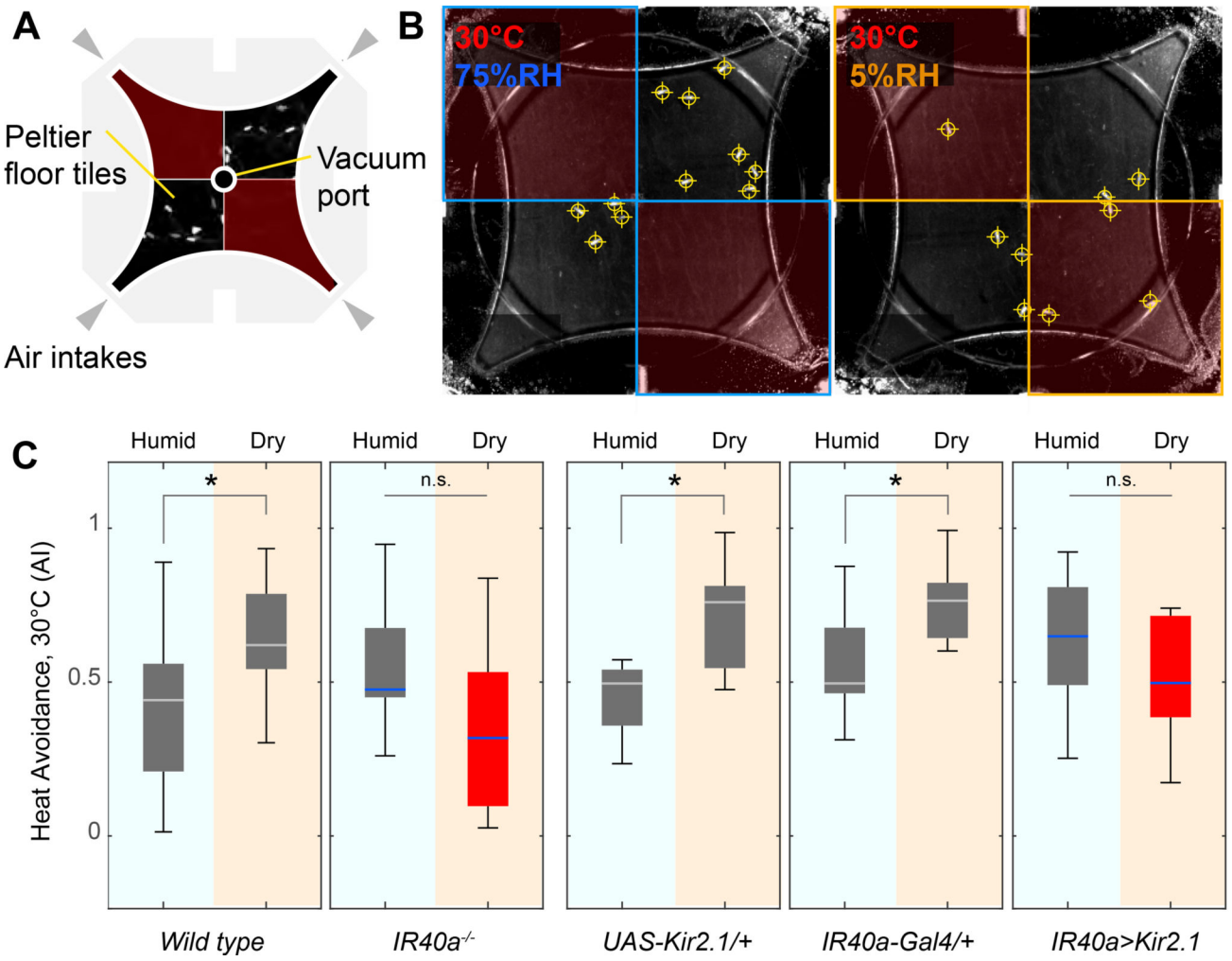

Figure 4. Hot and dry conditions synergize to mediate behavioral avoidance

(A,B) A new assay demonstrates the modulation of heat avoidance by either dry or humid air. (A) Assay design. A four-field olfactometer is mounted atop a chamber tiled by Peltier elements for temperature control. This allows independent control of RH/temperature in each quadrant. (B) Representative frames from a recording, annotated with the temperature of the floor tiles as well as the approximate RH in each quadrant (see methods for details, note that fly positions in this frame are shown as crosshairs).

(C) In this assay, behavioral avoidance of 30°C is significantly increased in the presence of dry air (see wild type and genetic controls, grey boxes; n= 5–10 trials, $p<0.05$, 2 sample t-test). This effect is abolished in *Ir40* mutants (*Ir40*^{1}) and in animals in which Ir40-expressing neurons are silenced by transgenic expression of Kir2.1 (red boxes, in all boxplots, the edges of the boxes are the first and third quartiles, thick lines mark the medians, and whiskers represent data range, n.s.=no significant difference $p>0.05$, 2 sample t-test; see Figure S3 for additional controls).

KEY RESOURCES TABLE

REAGENT or RESOURCE	SOURCE	IDENTIFIER
Antibodies		
rabbit anti-GFP	Life Technologies	Cat#A-11122; RRID:AB_221569
chicken anti-GFP	Abcam	Cat#ab13970; RRID:AB_300798
rabbit anti-IR25a	Ref. 5	N/A
guinea pig anti-IR40a	Gift from R. Benton	N/A
mouse anti-nc82	DSHB	Cat#nc82; RRID:AB_2314865
goat anti-rabbit Alexa 488	Life Technologies	Cat#A-11070; RRID:AB_2534114
goat anti-chicken Alexa 488	Life Technologies	Cat#A-11039; RRID:AB_2534096
goat anti-rabbit Alexa 594	Life Technologies	Cat#A-11037; RRID:AB_2534095
goat anti-guinea pig Alexa 546	Life Technologies	Cat#A-11074; RRID:AB_2534118
donkey anti-mouse Cy3	Jackson ImmunoResearch Labs	Cat#715-165-150; RRID:AB_2340813
Bacterial and Virus Strains		
Biological Samples		
Chemicals, Peptides, and Recombinant Proteins		
Rapiclear 1.47	SunJin Lab	Cat#RC147001
LiCl	Sigma- Aldrich	Cat#L9650
NaCl	Sigma- Aldrich	Cat#S9625
Critical Commercial Assays		
Deposited Data		
Experimental Models: Cell Lines		
Experimental Models: Organisms/Strains		
D. melanogaster $w^{1118\ CS}$	Gift from A. Simon	N/A
D. melanogaster: IR40a^{1}	Gift from R. Benton	N/A
D. melanogaster: IR68a^{MB05565}	Bloomington Drosophila Stock Center	BDSC:26031 Flybase: FBst0026031
D. melanogaster: IR40a-Gal4	Bloomington Drosophila Stock Center	(BDSC 41727) Flybase: FBst0041727

REAGENT or RESOURCE	SOURCE	IDENTIFIER
D. melanogaster: Ir40a-LexA	Gift from R. Benton	N/A
D. melanogaster: VT029048-Gal4	Vienna Drosophila Resource Center	VDRC: 207464 Flybase: FBst0486274
D. melanogaster: Ir93a-LexA	Ref. 9	N/A
D. melanogaster: IR25a-Gal4	Bloomington Drosophila Stock Center	BDSC:41728 Flybase: FBst0041728
D. melanogaster: 10XUAS-IVS-mCD8::GFP	Bloomington Drosophila Stock Center	BDSC:32186 Flybase: FBst0032186
D. melanogaster: 20XUAS-IVS-GCaMP6m	Bloomington Drosophila Stock Center	BDSC:42748 Flybase: FBst0042748
D. melanogaster: 13XLexAop-IVS-GCaMP6m	Bloomington Drosophila Stock Center	BDSC:44275 Flybase: FBst0044275
D. melanogaster: R22C06-Gal4	Bloomington Drosophila Stock Center	BDSC:48974 Flybase: FBst0048974
D. melanogaster: R24G07-Gal4	Bloomington Drosophila Stock Center	BDSC:49095 Flybase: FBst0049095
D. melanogaster: R24G07-LexA	Bloomington Drosophila Stock Center	BDSC:52726 Flybase: FBst0052726
D. melanogaster: UAS-syb:spGFP 1–10, AOP-CD4:spGFP 11	Bloomington Drosophila Stock Center	BDSC:64314 Flybase: FBst0064314
D. melanogaster: UAS-Kir2.1	Ref. 12	N/A
Oligonucleotides		
Recombinant DNA		
pENTR (pCR™8/GW/TOPO®)	Thermo Fisher Scientific	Cat#K250020
pBPLexAp65Uw	Ref. 10	Addgene Plasmid #26231
pJFRC19-13XLexAop2-IVS-myr::GFP	Ref. 10	Addgene Plasmid #26224
R22C06-LexAp65 (in *pBPLexAp65Uw*)	This paper	N/A
pJFRC19-*13XLexAop-TdTomato* in (*pJFRC19* backbone)	This paper	N/A
Software and Algorithms		
MATLAB	The MathWorks, Inc.	http://www.mathworks.com
Fiji		http://fiji.sc
Other		